

# Examination of Cobalt “Picket Fence” Porphyrin and Its Complex with 1-Methylimidazole as Catalysts for the Electroreduction of Dioxygen

Beat Steiger and Fred C. Anson\*

Arthur Amos Noyes Laboratories, Division of Chemistry and Chemical Engineering, California Institute of Technology, Pasadena, California 91125

Received May 22, 2000

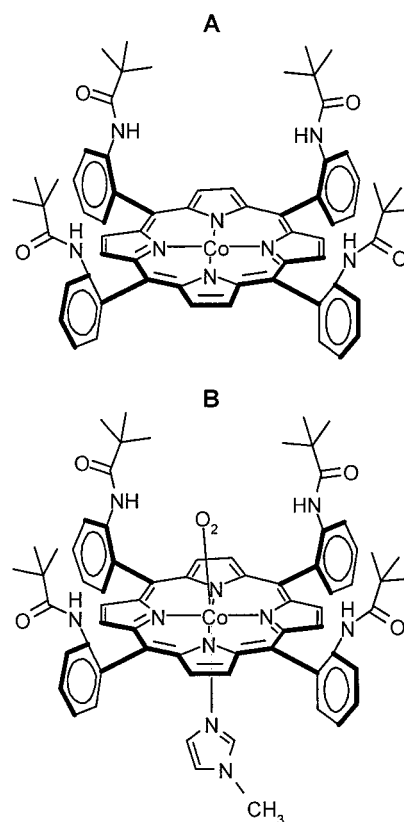
The electrochemical behavior of cobalt 5,10,15,20-tetrakis( $\alpha,\alpha,\alpha,\alpha$ -2-pivalamidophenyl)porphyrin ( $\text{Co}^{\text{II}}$ TpivPP) was examined in benzonitrile solutions. The electrochemical responses were changed significantly by the addition of 1-methylimidazole which coordinates once to the  $\text{Co}(\text{II})$  and twice to the  $\text{Co}(\text{III})$  porphyrin. The corresponding equilibrium binding constants were estimated as  $2.9 \times 10^3 \text{ M}^{-1}$  and  $1.7 \times 10^{20} \text{ M}^{-2}$ . The cyclic voltammetric responses were affected by the rates of the ligand association/dissociation reactions. Formation of the  $\text{O}_2$  adduct of the  $\text{Co}(\text{II})$  porphyrin resulted in only small changes in the cyclic voltammetric pattern. Comparison between  $\text{Co}^{\text{II}}$ TpivPP and cobalt tetraphenylporphyrin ( $\text{Co}^{\text{II}}$ TPP) as catalysts for the electroreduction of  $\text{O}_2$  showed the latter to be the superior catalyst both when adsorbed on graphite electrodes and when dissolved in thin layers of acidified benzonitrile where  $\text{Co}^{\text{II}}$ TpivPP exhibited unimpressive catalytic activity compared with  $\text{Co}^{\text{II}}$ TPP, which appeared to catalyze the reduction of  $\text{O}_2$  by significantly more than 2 electrons per molecule.

## Introduction

Cobalt porphyrins have been extensively investigated as catalysts for the electroreduction of dioxygen in aqueous solution.<sup>1</sup> The catalysis can be homogeneous when water-soluble porphyrins are employed, or heterogeneous when insoluble porphyrins are adsorbed (or otherwise immobilized) on the surfaces of electrodes. The mechanism that leads to the catalytic reduction is believed to commence with the coordination of  $\text{O}_2$  to the cobalt(II) center of the metalloporphyrin.<sup>1–3</sup> However, the evidence supporting this mechanism is largely circumstantial because the quantity of  $\text{Co}(\text{II})\text{--O}_2$  adduct formed in aqueous solution is typically too small to be observed. That enhanced rates of reduction of  $\text{O}_2$  are nevertheless observed is usually attributed to the high electrochemical reactivity of the  $\text{Co}(\text{II})\text{--O}_2$  adduct and its ready reformation during the catalytic cycle.

With the objective of observing the catalytically important  $\text{Co}(\text{II})\text{--O}_2$  adduct directly, we were drawn to the cobalt “picket fence” porphyrin, 5,10,15,20-tetrakis( $\alpha,\alpha,\alpha,\alpha$ -2-pivalamidophenyl)porphyrin ( $\text{Co}^{\text{II}}$ TpivPP), of Collman et al.<sup>4</sup> (Chart 1) because of its unique ability to form substantial concentrations of a  $\text{Co}(\text{II})\text{--O}_2$  adduct at room temperature in hydrocarbon solvents.<sup>4</sup> The electrochemical behavior of  $\text{Co}^{\text{II}}$ TpivPP and its  $\text{O}_2$  adduct have not been previously explored in detail. We found that, in addition to its formation in hydrocarbons, the adduct could also be formed in common electrochemical solvents. Using benzonitrile (BN) as solvent and 1-methylimidazole (1-MeIm) as axial base, it was possible to discern some of the

**Chart 1.** Structures of Cobalt “Picket Fence” Porphyrin ( $\text{Co}^{\text{II}}$ TpivPP) (A) and the Adduct of  $\text{Co}^{\text{II}}$ TpivPP with  $\text{O}_2$  with 1-Methylimidazole as the Axial Base (B)



\* Corresponding author. E-mail: fanson@caltech.edu. Telephone: (626) 395-6000. Fax: (626) 577-4088.

- (1) (a) Yeager, E. *Electrochim. Acta* **1984**, *29*, 1527–1537 and references therein. (b) Anson, F. C.; Shi, C.; Steiger, B. *Acc. Chem. Res.* **1997**, *30*, 437–444 and references therein.
- (2) Ni, C.-L.; Anson, F. C. *Inorg. Chem.* **1985**, *24*, 4754–4756 and references therein.
- (3) Shi, C.; Anson, F. C. *J. Am. Chem. Soc.* **1991**, *113*, 9564–9570.
- (4) Collman, J. P.; Braumann, J. I.; Doxsee, K. M.; Halbert, T. R.; Hayes, S. E.; Suslick, K. S. *J. Am. Chem. Soc.* **1978**, *100*, 2761–2766.

electrochemical properties of the  $(1\text{-MeIm})\text{Co}^{\text{II}}(\text{O}_2)$  adduct. A small response attributed to the reduction of the coordinated  $\text{O}_2$  was observed.

This report summarizes the results obtained including equilibrium constants for the binding of 1-MeIm and  $\text{O}_2$  to  $\text{Co}^{\text{II}}$ .

TpivPP in benzonitrile and a comparison of  $\text{Co}^{\text{II}}$ TpivPP with cobalt tetraphenylporphyrin ( $\text{Co}^{\text{II}}$ TPP) as catalysts for the electroreduction of  $\text{O}_2$ . The four molecular "pickets" that are appended to one side of the porphyrin ring in  $\text{Co}^{\text{II}}$ TpivPP, and that are responsible for the unusually high affinity for  $\text{O}_2$  of the 1-MeIm complex of the porphyrin, appear to hinder (rather than to enhance) its catalytic activity toward the electroreduction of  $\text{O}_2$ .

### Experimental Section

**Materials.** The synthesis of the "picket fence" porphyrin, 5,10,15,20-tetrakis( $\alpha,\alpha,\alpha,\alpha$ -2-pivalamidophenyl)porphyrin, and its metalation with  $\text{Co}(\text{II})$  were accomplished by procedures similar to those of Collman et al.<sup>4</sup> as described in a recent report.<sup>5</sup> Cobalt 5,10,15,20-tetraphenylporphyrin ( $\text{Co}^{\text{II}}$ TPP) was prepared according to procedures in the literature.<sup>6–8</sup> Other high-purity reagents were obtained from commercial sources and used as received except for benzonitrile (BN), which was purified by passage through a column of activated Linde 3A molecular sieves followed by distillation under reduced pressure.

**Apparatus and Procedures.** Conventional electrochemical cells and instrumentation were employed. Glassy carbon (GC) working electrodes from Bioanalytical Systems were polished with 0.05 mm alumina before use. Edge plane pyrolytic graphite (EPG) electrodes from Advanced Ceramics Corp. were polished on 600 grit SiC paper followed by sonication in water. The coordination of 1-MeIm by  $\text{Co}^{\text{II}}$ TpivPP in BN saturated with argon was monitored spectrophotometrically following conventional procedure.<sup>9,10</sup> An equilibrium association constant of  $2.6 \times 10^3 \text{ M}^{-1}$  was estimated from the spectral data.

The coordination of  $\text{O}_2$  by (1-MeIm) $\text{Co}^{\text{II}}$ TpivPP was followed spectrophotometrically<sup>4</sup> in solutions containing sufficient 1-MeIm to convert essentially all of the  $\text{Co}^{\text{II}}$ TpivPP into (1-MeIm) $\text{Co}^{\text{II}}$ TpivPP. The equilibrium constant for the coordination of  $\text{O}_2$  by (1-MeIm) $\text{Co}^{\text{II}}$ TpivPP obtained from the spectrophotometric data was  $\sim 3.9 \text{ (atm)}^{-1}$  at 25 °C and  $\sim 9.4 \text{ (atm)}^{-1}$  at 5 °C.

Except where otherwise noted, electrochemical experiments were conducted at the ambient laboratory temperature ( $22 \pm 2$  °C). Reference electrodes employed were a saturated calomel electrode (SCE), an aqueous  $\text{Ag}/\text{AgCl}/3 \text{ M NaCl}$  reference electrode ( $-40 \text{ mV vs SCE}$ ) or a sodium chloride saturated calomel electrode, SSCE ( $5 \text{ mV vs SCE}$ ).

Thin layers of BN separating polished EPG electrodes from aqueous electrolyte solutions were prepared and utilized according to procedures that have been described.<sup>11</sup> Supporting electrolyte ( $\text{HClO}_4$ ) partitioned into the thin layers from the aqueous supporting electrolyte solutions. The quantities of  $\text{HClO}_4$  that partitioned into BN from aqueous solutions of the acid were determined by titration of aliquots of the BN phase with standard solutions of  $\text{NaOH}$ .

### Results

**Cyclic Voltammetry of  $\text{Co}^{\text{II}}$ TpivPP.**  $\text{Co}^{\text{II}}$ TpivPP exhibited the same pattern of voltammetric responses in a variety of organic solvents. The data in this report were obtained using BN because of the good solubility of the porphyrin in this solvent (even below room temperature). In addition, the low volatility of BN facilitated the formation of stable thin layers of the solvent on the surface of graphite electrodes.

Shown in Figure 1A is a cyclic voltammogram for a solution of  $\text{Co}^{\text{II}}$ TpivPP in BN. Two reversible responses were obtained

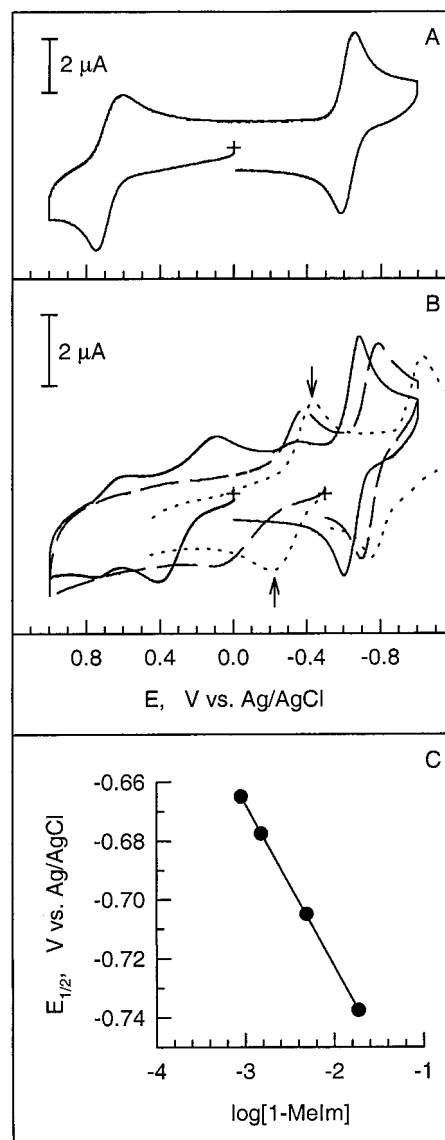


**Figure 1.** (A) Cyclic voltammetry of 0.5 mM  $\text{Co}^{\text{II}}$ TpivPP in benzonitrile (BN). The initial electrode potential was 0 V. Scan rate:  $50 \text{ mV s}^{-1}$ . Supporting electrolyte: 0.1 M tetrabutylammonium perchlorate (TBAP). Glassy carbon electrode ( $0.07 \text{ cm}^2$ ). (B) Repeat of A in the presence of 1-MeIm. The concentrations of 1-MeIm and the initial electrode potentials were (solid curve) 0.2 mM, 0 V; (dashed curve) 19 mM,  $-0.6 \text{ V}$ ; and (dotted curve) 1.4 M,  $-0.6 \text{ V}$ . (C) Dependence of the average of the cathodic and anodic peak potentials ( $E_{1/2}$ ) of the  $\text{Co}(\text{II/I})$  response on the concentration of 1-MeIm.

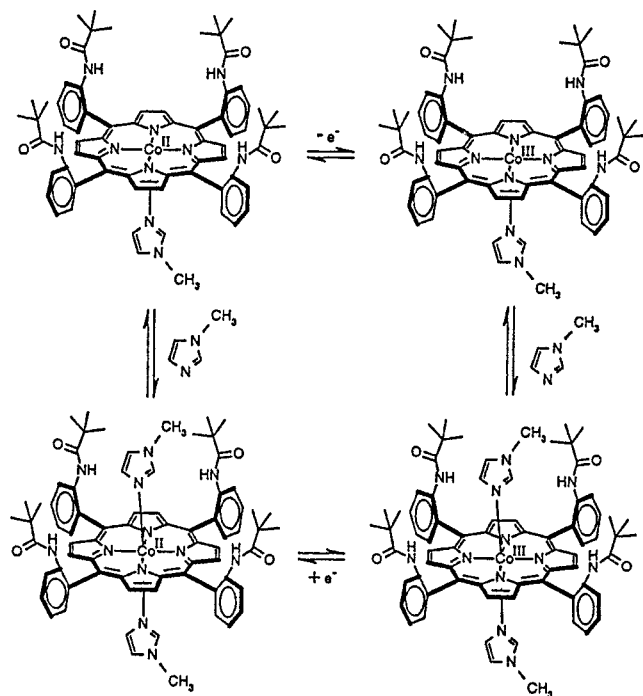
at 0.68 and  $-0.62 \text{ V}$  that can be assigned to the  $\text{Co}(\text{III/II})$  and the  $\text{Co}(\text{II/I})$  couples, respectively. These assignments are based on the similarity of the responses to those obtained with other cobalt porphyrins.<sup>12</sup>

**Effect of 1-Methylimidazole on the Voltammetry.** The affinity of  $\text{Co}^{\text{II}}$ TpivPP for  $\text{O}_2$  is enhanced substantially by coordination of a suitable base in the axial coordination site on the unencumbered side of the porphyrin ring.<sup>4</sup> 1-MeIm is particularly effective for this purpose, so it was important to examine the effect of 1-MeIm on the electrochemistry of  $\text{Co}^{\text{II}}$ TpivPP (at first, in the absence of  $\text{O}_2$ ). Upon coordination to the cobalt center, 1-MeIm causes the voltammetric responses for both the  $\text{Co}(\text{III/II})$  and the  $\text{Co}(\text{II/I})$  couples to shift to more negative potentials. Shown in Figure 1B are cyclic voltammo-

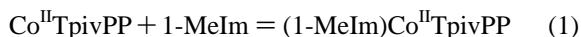
- (5) Steiger, B.; Baskin, J. S.; Anson, F. C.; Zewail, A. H. *Angew. Chem., Int. Ed.* **2000**, *39*, 257–260.
- (6) Adler, A. D.; Longo, F. R.; Finarelli, J. D.; Goldmacher, J.; Assour, J.; Korsakoff, L. *J. Org. Chem.* **1967**, *32*, 476.
- (7) Barnett, G. H.; Hudson, M. F.; Smith, K. M. *Tetrahedron Lett.* **1973**, 2887–2888.
- (8) Adler, A. D.; Longo, F. R.; Kampas, F.; Kim, J. *J. Inorg. Nucl. Chem.* **1970**, *32*, 2443–2445.
- (9) Rose, N. J.; Drago, R. S. *J. Am. Chem. Soc.* **1959**, *81*, 6138–6145.
- (10) Drago, R. S. *Physical Methods in Chemistry*; W. B. Saunders: Philadelphia, PA, 1977; p 88.
- (11) Shi, C.; Anson, F. C. *Anal. Chem.* **1998**, *70*, 3114–3118.

- (12) Kadish, K. M. *Prog. Inorg. Chem.* **1986**, *34*, 435–605.

Scheme 1



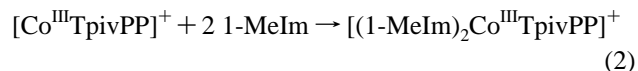
grams for  $\text{Co}^{\text{II}}\text{TpivPP}$  in the presence of 1-MeIm. The responses obtained differ in three important respects from that shown in Figure 1A: (i) The oxidation of the Co(II) porphyrin occurs over a broad potential range ( $-0.4$  to  $+0.6$  V), and the position of the anodic response is very sensitive to the concentration of 1-MeIm. The anodic peaks are less sharp than the single anodic peak in Figure 1A, and they appear to involve more than a single electrode reaction. (ii) The Co(III) products of the oxidation give rise to several cathodic peaks with positions and magnitudes that depend upon the concentration of 1-MeIm. (iii) The response from the Co(II/I) couple lies in the range between  $-0.7$  and  $-1.1$  V and is not split into multiple peaks. The average of the cathodic and anodic peak potentials for the Co(II/I) couple shifts to more negative values as the concentration of 1-MeIm increases. The shift amounts to about 55 mV per decadic change in the concentration of 1-MeIm (Figure 1C), indicating that one more 1-MeIm ligand is coordinated to  $\text{Co}^{\text{II}}\text{TpivPP}$  than to  $[\text{Co}^{\text{I}}\text{TpivPP}]^-$ . With toluene as solvent, it is known that  $\text{Co}^{\text{II}}\text{TpivPP}$  coordinates only one 1-MeIm.<sup>4</sup> It is therefore highly likely that no 1-MeIm is coordinated to  $[\text{Co}^{\text{I}}\text{TpivPP}]^-$  in BN. An equilibrium constant of  $2.9 \times 10^3 \text{ M}^{-1}$  (at 25 °C) for reaction 1 in BN (containing 0.1 M tetrabutylammonium perchlorate (TBAP)) was calculated from the shift of  $-0.12$  V in the formal potential of the Co(II/I) couple caused by the presence of 37.5 mM 1-MeIm. Analogous experiments at 5 °C and 2.5 mM



1-MeIm yielded an equilibrium constant of  $6.4 \times 10^3 \text{ M}^{-1}$ . The value at 25 °C is comparable to that evaluated spectrophotometrically ( $K = 2.6 \times 10^3 \text{ M}^{-1}$ ), but it is smaller than the value reported<sup>4</sup> with toluene as the solvent and in the absence of supporting electrolyte ( $K = 1.7 \times 10^4 \text{ M}^{-1}$  at 20 °C).

To evaluate the corresponding equilibrium constant for the coordination of 1-MeIm to  $[\text{Co}^{\text{III}}\text{TpivPP}]^+$  it was necessary to obtain the formal potential of the Co(III/II) couple in the presence of 1-MeIm. The pattern of the voltammetric responses in Figure 1B suggests a mechanistic "square scheme" such as the one depicted in Scheme 1. If the rates of the coordination–

dissociation steps shown in Scheme 1 were sufficiently large, the response from the Co(III/II) couple would resemble that of the Co(II/I) couple. That is, the addition of 1-MeIm would cause the response near 0.68 V in Figure 1A to shift to more negative potentials but only one anodic and one cathodic peak would be present. The different pattern observed experimentally (Figure 1B) indicates that the coordination reactions in Scheme 1 proceed too slowly for equilibrium to be maintained during the recording of the cyclic voltammograms. However, with a sufficiently high concentration of the ligand, the Co(III/II) response more nearly resembles that of the Co(II/I) couple (Figure 1B) and the average of the resulting anodic and cathodic peak potentials (marked by arrows in Figure 1B) provides a reasonable approximation to the formal potential of the couple. A value of  $-0.32$  V was obtained in the presence of 1.4 M 1-MeIm. The significant negative shifts in the formal potential of the Co(III/II) couple caused by the addition of 1-MeIm show that the number of these ligands coordinated to  $[\text{Co}^{\text{III}}\text{TpivPP}]^+$  must exceed the number (one) coordinated to  $\text{Co}^{\text{II}}\text{TpivPP}$ . Since only two open coordination sites are available on  $\text{CoTpvPP}$  (Chart 1),  $[\text{Co}^{\text{III}}\text{TpivPP}]^+$  must coordinate two 1-MeIm ligands with one located inside the "picket fence" attached to the porphyrin ring. Using the shift in the formal potentials of the Co(III/II) couple caused by the presence of 1.4 M 1-MeIm, an equilibrium constant of  $1.7 \times 10^{20} \text{ M}^{-2}$  was calculated for reaction 2. The affinity of  $[\text{Co}^{\text{III}}\text{TpivPP}]^+$  for 1-MeIm molecules as axial ligands is clearly much greater than that of  $\text{Co}^{\text{II}}\text{TpivPP}$  ( $K = 2.9 \times 10^3 \text{ M}^{-1}$ ).



**Voltammetry of (1-MeIm)CoTpvPP(O<sub>2</sub>).** The addition of O<sub>2</sub> to solutions of  $\text{Co}^{\text{II}}\text{TpivPP}$  in BN containing 1-MeIm causes the formation of the (1-MeIm)CoTpvPP(O<sub>2</sub>) complex. The assignment of oxidation states to Co and O<sub>2</sub> in the complex is arbitrary (Co(II) and O<sub>2</sub> or Co(III) and O<sub>2</sub><sup>•-</sup>), but spectral evidence favors the Co(III)–O<sub>2</sub><sup>•-</sup> combination. In what follows we will not assign individual oxidation states in depicting the complex.

The changes in the cyclic voltammetry of (1-MeIm)Co<sup>II</sup>TpivPP that occur in the presence of O<sub>2</sub> are shown in Figure 2. The experiments were carried out at 5 °C where the coordination of O<sub>2</sub> is more extensive than at room temperature. In Figure 2A are voltammograms obtained when the electrode potential was scanned to more positive values from an initial potential of  $-0.6$  V. Before O<sub>2</sub> was introduced into the solution, the response resembled that in Figure 1B with the oxidation of (1-MeIm)Co<sup>II</sup>TpivPP proceeding as depicted in Scheme 1. The equilibration of the solution with first 0.2 and then 1.0 atm of O<sub>2</sub> converted first 66% and then 93% of the complex to the O<sub>2</sub> adduct and produced notable effects in the voltammetry: The broad response near 0.05 V was depressed as a new peak developed near 0.5 V. The pattern observed is consistent with a competition between O<sub>2</sub> and 1-MeIm for coordination to the cobalt center. The anodic response near 0.05 V corresponds to the generation of  $[(\text{1-MeIm})_2\text{Co}^{\text{III}}\text{TpivPP}]^+$  by oxidation of (1-MeIm)Co<sup>II</sup>TpivPP according to Scheme 1. In the presence of O<sub>2</sub> the site where the second 1-MeIm ligand coordinates is occupied by an O<sub>2</sub> molecule that must dissociate before the incoming 1-MeIm ligand can be accommodated. The diminished current near 0.05 V in the presence of O<sub>2</sub> indicates that this ligand substitution process is less facile than when the sixth coordination site on the Co(II) center is unoccupied (except,



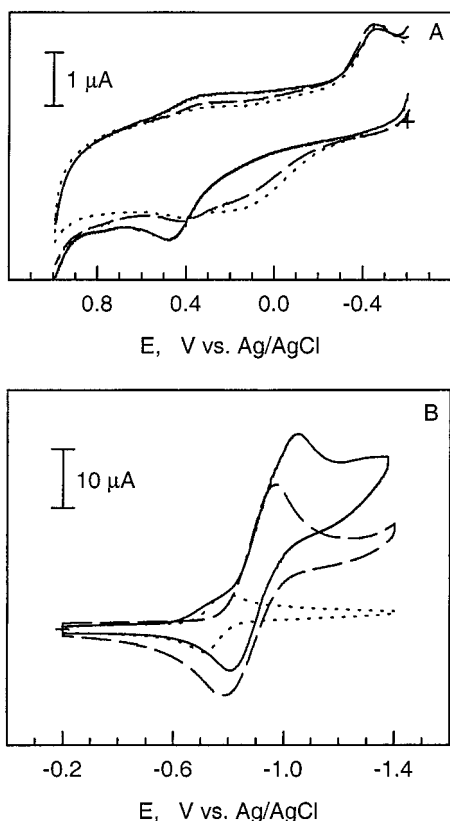


**Figure 2.** Effect of O<sub>2</sub> on the cyclic voltammetry of (1-MeIm)Co<sup>II</sup>-TpivPP. (A) Electrode potential scanned from -0.6 V toward more positive potentials in a BN solution containing 0.5 mM Co<sup>II</sup>TpivPP, 19 mM 1-MeIm, and 0.1 M tetrabutylammonium hexafluorophosphate. The solution was equilibrated with O<sub>2</sub> at partial pressures of (dotted curve) 0, (dashed curve) 0.2, and (solid curve) 1.0 atm. Scan rate: 50 mV s<sup>-1</sup>. Glassy carbon electrode (0.07 cm<sup>2</sup>). Solution temperature: 5 °C. (B) Electrode potential scanned from -0.2 V toward more negative potentials in a BN solution containing (dotted curve) 1.0 mM Co<sup>II</sup>-TpivPP + 3 mM 1-MeIm, (dashed curve) 3 mM 1-MeIm and equilibrated with 0.2 atm of O<sub>2</sub>, and (solid curve) 1.0 mM Co<sup>II</sup>-TpivPP + 3 mM 1-MeIm and equilibrated with 0.2 atm of O<sub>2</sub>. Other conditions as in panel A.

possibly, by a weakly bound solvent molecule). The new anodic peak near 0.5 V is believed to arise from the oxidation of the (1-MeIm)CoTpivPP(O<sub>2</sub>) complex. The initial oxidation product is eventually converted to [(1-MeIm)<sub>2</sub>Co<sup>III</sup>TpivPP]<sup>+</sup> (the species responsible for the cathodic peak near -0.4 V), but comparison with Figure 1B (dashed curve) shows that this ligand substitution at cobalt(III) is delayed as compared with the situation in the absence of O<sub>2</sub>.

The cathodic voltammetry of (1-MeIm)Co<sup>II</sup>TpivPP in the presence of O<sub>2</sub> is complicated by the fact that the reversible reduction of O<sub>2</sub> to O<sub>2</sub><sup>•-</sup> falls in the same potential range as the reduction of the porphyrin complex. Shown in Figure 2B are cyclic voltammograms for O<sub>2</sub> alone, for (1-MeIm)Co<sup>II</sup>TpivPP alone, and for a mixture of the two in a BN solution also containing 1-MeIm. Careful comparison of the solid and dotted curves near -0.75 V shows that the reduction of (1-MeIm)-CoTpivPP(O<sub>2</sub>) commences slightly before the reduction of (1-MeIm)Co<sup>II</sup>TpivPP. This reduction can occur at a potential less negative than that needed to reduce uncoordinated O<sub>2</sub> because of the stabilization of the reduction products, O<sub>2</sub><sup>•-</sup> and Co(II), provided by their coordination to each other. The subsequent reduction of uncoordinated O<sub>2</sub> appears not to be influenced by the presence of [Co<sup>I</sup>TpivPP]<sup>-</sup> at the electrode surface (compare the dashed and solid curves in Figure 2B), suggesting that the

anionic [Co<sup>I</sup>TpivPP]<sup>-</sup> complex has little affinity for O<sub>2</sub><sup>•-</sup>. The only feature in the cathodic voltammetry for the mixture in Figure 2B that differs from the sum of the responses of the two components of the mixture is the small wave at the foot of the solid curve.

**Comparison of the Electroreduction of O<sub>2</sub> as Catalyzed by Co<sup>II</sup>TpivPP or Co<sup>II</sup>TPP in the Presence of Protons.** The ability of a variety of cobalt porphyrins to serve as electrocatalyst for the reduction of O<sub>2</sub> in the presence of acid is well established.<sup>2</sup> Frequently, the catalyst is irreversibly adsorbed on the surface of graphite disk electrodes which are rotated in acidified solutions of O<sub>2</sub>. As the electrode potential is scanned to more negative values, the reduction of O<sub>2</sub> produces steady-state plateau currents with magnitudes that increase with the rate of rotation of the electrode. Shown in Figure 3A is a set of such current-potential curves for the reduction of O<sub>2</sub> at a rotating graphite disk electrode coated with Co<sup>II</sup>TPP. The presence of the Co<sup>II</sup>TPP on the electrode surface causes the reduction of O<sub>2</sub> to occur at significantly more positive potentials than is the case when an uncoated electrode is used (dashed curve in Figure 3A). The catalysis is reasonably efficient because there is no indication that unreduced O<sub>2</sub> remains at the electrode surface where it would be reduced at the more negative potentials observed with uncoated electrodes (dashed curve).

The behavior observed when the experiments of Figure 3A were repeated with Co<sup>II</sup>TpivPP adsorbed on the electrode is shown in Figure 3B. The reduction of O<sub>2</sub> occurs at about the same potential as with Co<sup>II</sup>TPP, but the increase of the plateau currents with the electrode rotation rate is significantly smaller. Levich plots<sup>13</sup> of the plateau currents vs (rotation rate)<sup>1/2</sup> with Co<sup>II</sup>TPP or Co<sup>II</sup>TpivPP as the adsorbed catalyst are shown in Figure 3C, where the insensitivity of the plateau currents to the rotation rate at the Co<sup>II</sup>TpivPP-coated electrode is evident. The pattern of behavior exhibited in Figure 3B,C is indicative of a mechanism in which a chemical step preceding the electrode reaction limits the magnitude of the plateau currents at the higher rotation rates. This step is most likely the coordination of O<sub>2</sub> to the Co(II) center of the adsorbed porphyrins. The rate of this coordination is evidently slower for Co<sup>II</sup>TpivPP than for Co<sup>II</sup>-TPP.

**Catalytic Reduction of O<sub>2</sub> within Thin Layers of BN at the Electrode Surface.** Further insight into the catalyzed reduction of O<sub>2</sub> was obtained by dissolving the porphyrin catalysts in a thin layer of BN next to the electrode instead of adsorbing them directly on the electrode surface. The utility of such adherent thin layers of organic solvents on electrode surfaces has been recently described.<sup>11</sup> In the present instance the thin layer methodology allowed readily measurable responses to be obtained for the reduction of O<sub>2</sub> in BN that was equilibrated with an aqueous solution of HClO<sub>4</sub> which partitioned into the BN layer to serve as the supporting electrolyte. Shown in Figure 4A are cyclic voltammograms obtained with an EPG electrode on which was placed a 30 μm layer of BN containing Co<sup>II</sup>TPP. The electrode was immersed in 2 M (aqueous) HClO<sub>4</sub>. The dashed curve is the response from the reversible Co(III/II) couple in the absence of O<sub>2</sub>. After the aqueous solution was saturated with air, the solid curve was obtained. The large peak results from the catalyzed reduction of the O<sub>2</sub> present in the air-saturated BN layer. (The concentration of O<sub>2</sub> in air-saturated BN is ca. 1.3 mM.) The initial reduction current decays to a pseudo-steady-state value that is controlled by the rate at which O<sub>2</sub> can be supplied to the BN

(13) Levich, V. G. *Physicochemical Hydrodynamics*; Prentice Hall: Englewood Cliffs, NJ, 1962.

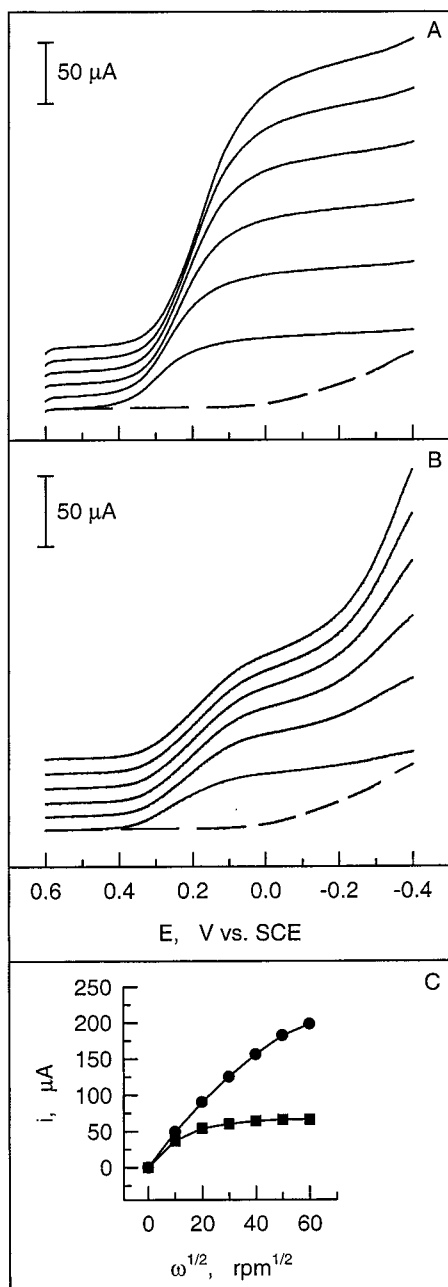


**Figure 3.** Current-potential curves for the electroreduction of  $O_2$  at a rotating graphite disk electrode coated with  $2 \times 10^{-9}$  mol  $cm^{-2}$  of (A)  $Co^{II}TPP$  or (B)  $Co^{II}TpvPP$ . Supporting electrolyte: 0.5 M  $HClO_4$  + 0.5 M  $NH_4PF_6$  (previously shown to help stabilize porphyrin coatings on electrodes) saturated with air. Electrode rotation rates (bottom to top): 100, 400, 900, 1600, 2500, 3600 rpm. Potential scan rate:  $5 \text{ mV s}^{-1}$ . The dashed curves were obtained with the uncoated electrode at a rotation rate of 100 rpm. (C) Levich plots of the plateau currents of A (●) and B (■) vs (rotation rate) $^{1/2}$ .

layer by diffusion and partitioning from the aqueous solution where the concentration of  $O_2$  is only 0.28 mM. The catalytic efficiency of the  $Co^{II}TPP$  dissolved in the BN layer is evidently reasonably high as judged by the absence of a second cathodic peak at the potential where the uncatalyzed reduction of  $O_2$  proceeds (dotted curve in Figure 4A).

The catalyzed reduction of  $O_2$  begins at the same potential where the  $[Co^{III}TPP]^+$  is reduced to  $Co^{II}TPP$ . This correspondence indicates that the  $CoTPP(O_2)$  adduct (presumed to be the reactive intermediate in the catalytic cycle) is reduced at potentials no less positive than 0.25 V. In the absence of

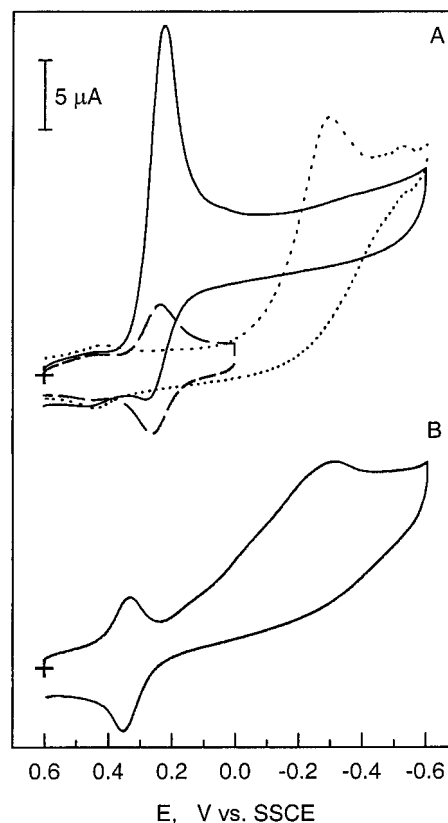


**Figure 4.** Cyclic voltammetry of  $Co^{II}TPP$  and  $Co^{II}TpvPP$  dissolved in thin layers of acidified BN in the presence of  $O_2$ . (A) 1.8 mM  $Co^{II}TPP$  in a  $30 \mu\text{m}$  thin layer of BN placed on an EPG electrode ( $0.32 \text{ cm}^2$ ) that was immersed in 2 M aqueous  $HClO_4$ . Dashed curve: in the absence of  $O_2$ . Solid curve: after the aqueous phase (and the equilibrated thin layer of BN) was saturated with air. Scan rate:  $5 \text{ mV s}^{-1}$ . The concentration of  $HClO_4$  in the equilibrated thin layer of BN was ca. 25 mM. The dotted curve is the response obtained for the reduction of  $O_2$  when the BN layer contained no porphyrin. (B) As for the solid curve in panel A except that 1.9 mM  $Co^{II}TpvPP$  was used in place of  $Co^{II}TPP$ .

$Co^{II}TPP$  the reduction of  $O_2$  occurs near  $-0.3 \text{ V}$  (dotted curve in Figure 4A). The positive shift of 0.55 V in the potential where  $O_2$  is reduced reflects the catalytic potency of  $Co^{II}TPP$  in acidified BN.

The charge represented by the flow of the pseudo-steady-state current of ca.  $10 \mu\text{A}$  in Figure 4A for 140 s amounts to ca.  $1400 \mu\text{C}$ . The maximum quantity of  $O_2$  that could diffuse to the BN/ $H_2O$  interface during this time period from the 0.28 mM solution can be calculated as  $4.9 \times 10^{-9}$  mol. The reduction of this quantity of  $O_2$  would consume  $480 \mu\text{C}$  per electron involved in the reduction. Comparison of this value with the experimentally observed value of  $1400 \mu\text{C}$  indicates that the  $O_2$  is reduced by significantly more than 2 electrons per molecule. When adsorbed on the surface of EPG electrodes,  $Co^{II}TPP$  catalyzes the reduction of  $O_2$  only to  $H_2O_2$ .<sup>14</sup> Its apparent ability to carry the reduction beyond  $H_2O_2$  in acidified BN is noteworthy. Additional tests are called for to determine how general this novel behavior may be.

The measurements of Figure 4A were repeated with  $Co^{II}TpvPP$  dissolved in the BN layer, and the response obtained is shown in Figure 4B.  $Co^{II}TpvPP$  is a considerably weaker catalyst than  $Co^{II}TPP$ : The catalyzed reduction begins only at more negative potentials than that where  $[Co^{III}TpvPP]^+$  is

(14) Song, E.; Shi, C.; Anson, F. C. *Langmuir* **1998**, *14*, 4315-4321.

reduced to  $\text{Co}^{\text{II}}\text{TpivPP}$ , and the wave for the reduction of  $\text{O}_2$  is more drawn out and overlaps the wave for the uncatalyzed reduction of  $\text{O}_2$  (dotted curve in Figure 4A). The implication is that the  $\text{CoTpvPP}(\text{O}_2)$  complex is less reactive or is formed more slowly than  $\text{CoTPP}(\text{O}_2)$ , or both. Thus,  $\text{Co}^{\text{II}}\text{TPP}$  exhibits greater catalytic activity than does  $\text{Co}^{\text{II}}\text{TpvPP}$  toward the reduction of  $\text{O}_2$  in the presence of acid both when the two porphyrins are adsorbed on graphite electrodes (Figure 3) and when they are dissolved in acidified BN (Figure 4).

## Discussion

**Electrochemistry of  $\text{Co}^{\text{II}}\text{TpvPP}$ .** The attachment of the pivalamido "pickets" to the four phenyl rings of  $\text{Co}^{\text{II}}\text{TPP}$  does not result in significant changes in the voltammetric responses from the  $\text{Co}(\text{III}/\text{II})$  or  $\text{Co}(\text{II}/\text{I})$  couples of the porphyrin in BN. Except for a positive shift in formal potentials, nothing in the response shown in Figure 1A for  $\text{Co}^{\text{II}}\text{TpvPP}$  distinguishes it from that exhibited by  $\text{Co}^{\text{II}}\text{TPP}$  in the same solvent. However, Saveant et al.<sup>15</sup> have shown that in solvents such as 1,2-dichloroethane a 2-electron oxidation of the TpvPP ligand occurs to produce an internal isoporphyrin. The oxidation of the cobalt(II) center of  $\text{Co}^{\text{II}}\text{TpvPP}$  occurs near the same potential so that a net 3-electron anodic peak is observed in 1,2-dichloroethane solutions of  $\text{Co}^{\text{II}}\text{TpvPP}$ .<sup>16</sup> That this pattern of reactivity is not seen in BN solutions reflects the greater coordinating ability of BN which shifts the potential of the  $\text{Co}(\text{III}/\text{II})$  couple to less positive values (Figure 1A) where no oxidation of the TpvPP ligand accompanies the oxidation of the cobalt center.

**Coordination of 1-MeIm by  $\text{Co}^{\text{II}}\text{TpvPP}$  in BN.** The coordination of one and only one molecule of 1-MeIm by  $\text{Co}^{\text{II}}\text{TpvPP}$  in BN, as indicated by the data in Figure 1C, conforms with its behavior in toluene solutions.<sup>4</sup> The  $\sim 6$ -fold smaller equilibrium constant for the coordination in BN presumably reflects the greater nucleophilicity of BN which can compete with 1-MeIm to occupy the coordination site. The fact that a 1-MeIm ligand does not enter the cavity defined by the four "pickets" on one side of the porphyrin ring of  $\text{Co}^{\text{II}}\text{TpvPP}$  is probably a reflection of a steric barrier imposed by the pickets. However, the ligand is strongly bound to both axial coordination sites in  $[\text{Co}^{\text{III}}\text{TpvPP}]^+$  (reaction 2) so the steric barrier is not insurmountable. The significantly lower intrinsic affinity of  $\text{Co}(\text{II})$  for the 1-MeIm ligand must account for the lack of formation of  $(1\text{-MeIm})_2\text{Co}^{\text{II}}\text{TpvPP}$ , at least at ligand concentrations below  $\sim 1$  M. The low affinity of  $(1\text{-MeIm})\text{Co}^{\text{II}}\text{TpvPP}$  for a second 1-MeIm ligand facilitates the formation of the  $\text{O}_2$  complex,  $(1\text{-MeIm})\text{CoTpvPP}(\text{O}_2)$ , in which the electron in the  $d_{z^2}$  orbital of the  $\text{Co}(\text{II})$  center can participate in the bonding to the coordinating  $\text{O}_2$  molecule.

The multiple anodic and subsequent cathodic peaks that result when 1-MeIm is added to solutions of  $\text{Co}^{\text{II}}\text{TpvPP}$  before it is anodically oxidized (Figure 1B) suggest a "square scheme" such as the one shown in Scheme 1. The anodic oxidation of  $(1\text{-MeIm})\text{Co}^{\text{II}}\text{TpvPP}$  induces the coordination of a second ligand to produce the ultimate product,  $[(1\text{-MeIm})_2\text{Co}^{\text{III}}\text{TpvPP}]^+$ , but the electron-transfer and ligand association steps are evidently not concerted. The delay in the coordination step is not attributable to the presence of the molecular "pickets" because a voltammetric pattern like the one shown in Figure 1B is also obtained when  $\text{Co}^{\text{II}}\text{TPP}$  is oxidized in the presence of 1-MeIm.<sup>16</sup>

The behavior exhibited by both cobalt porphyrins suggests that the displacement of BN on the  $\text{Co}(\text{III})$  center by 1-MeIm may be the slow step.

Once the concentration of 1-MeIm exceeds a few millimolar, the position of the cathodic peak for the reduction of  $[(1\text{-MeIm})_2\text{Co}^{\text{III}}\text{TpvPP}]^+$  (marked by the upper arrow in Figure 1B) is affected only slightly by further increases in the concentration of the ligand. This behavior indicates that the decomposition of the product of the reduction,  $(1\text{-MeIm})_2\text{Co}^{\text{II}}\text{TpvPP}$ , into its stable form,  $(1\text{-MeIm})\text{Co}^{\text{II}}\text{TpvPP}$ , is not rapid.

The absence of evidence of slow coordination steps during the reduction of  $(1\text{-MeIm})\text{Co}^{\text{II}}\text{TpvPP}$  (and the subsequent oxidation of  $[\text{Co}^{\text{I}}\text{TpvPP}]^-$  indicates that the dissociation of the single 1-MeIm ligand from  $\text{Co}(\text{I})$  is more rapid than from  $\text{Co}(\text{II})$ ; and during the oxidation of the four-coordinate  $\text{Co}(\text{I})$  complex there is no impediment to the rapid re-entry of the ligand to the unoccupied coordination site. As pointed out by a reviewer, the observed pattern of 2, 1, 0 axial ligands for the  $\text{Co}(\text{III},\text{II},\text{I})$  porphyrins echoes the coordination behavior of the cobalt center in vitamin B-12.<sup>17</sup>

The shifts in the formal potentials of the  $\text{Co}(\text{III}/\text{II})$  and  $\text{Co}(\text{II}/\text{I})$  couples of  $\text{CoTPP}$  in the presence of 1-MeIm correspond to equilibrium constants of ca.  $6 \times 10^2 \text{ M}^{-1}$  and  $1 \times 10^{19} \text{ M}^{-2}$  for the coordination reactions analogous to reactions 1 and 2, respectively.<sup>16</sup> The somewhat stronger association of 1-MeIm with  $[\text{Co}^{\text{III}}\text{TpvPP}]^+$  than with  $[\text{Co}^{\text{III}}\text{TPP}]^+$  may indicate a higher electron affinity of the former complex as reflected in its more positive formal potential. There is no corresponding difference in formal potentials for the two  $\text{Co}(\text{II}/\text{I})$  couples, and the equilibrium constants for the binding of 1-MeIm to the  $\text{Co}(\text{II})$  porphyrins do not differ greatly.

**Electrochemistry of  $(1\text{-MeIm})\text{CoTpvPP}(\text{O}_2)$ .** The coordination of  $\text{O}_2$  by  $(1\text{-MeIm})\text{Co}^{\text{II}}\text{TpvPP}$  produces only small changes in its electrochemical response (Figure 2). The coordinated  $\text{O}_2$  apparently adds to the delay in the rate of addition of a second 1-MeIm ligand to the oxidized ( $\text{Co}(\text{III})$ ) porphyrin (Figure 2A), and the small wave at the foot of the solid curve in Figure 2B was proposed to arise from the reduction of the  $(1\text{-MeIm})\text{CoTpvPP}(\text{O}_2)$  complex. The reduction of  $\text{O}_2$  to  $\text{O}_2^{\cdot-}$  is diffusion-controlled in BN and, therefore, not subject to catalysis. In the presence of protons or metal ions that react with  $\text{O}_2^{\cdot-}$ , catalysis of the reduction of  $\text{O}_2$  does occur to produce different reduction products:  $\text{H}_2\text{O}_2$  or metal- $\text{O}_2^{\cdot-}$  complexes.<sup>18</sup> The results shown in Figure 2B indicate that, however one may choose to assign oxidation states within  $(1\text{-MeIm})\text{CoTpvPP}(\text{O}_2)$ , its reduction takes place at a potential more positive than that where the reversible reduction of  $\text{O}_2$  to  $\text{O}_2^{\cdot-}$  occurs.

$\text{Co}^{\text{II}}\text{TpvPP}$  exhibits some activity as a catalyst for the reduction of  $\text{O}_2$  in the presence of acid. However, both when adsorbed on graphite electrodes (Figure 3) and when dissolved in a thin layer of acidified BN (Figure 4), it is a less effective catalyst than  $\text{Co}^{\text{II}}\text{TPP}$ . Thus, under conditions (necessarily nonacidic) where substantial quantities of the  $(1\text{-MeIm})\text{-CoTpvPP}(\text{O}_2)$  complex are formed, there is only a small positive shift in the potential where the reduction of  $\text{O}_2$  proceeds. In acidified media, where 1-MeIm  $\text{H}^+$  is not coordinated by  $\text{Co}^{\text{II}}\text{TpvPP}$ , the formation (of much smaller quantities) of a reductively reactive  $\text{CoTpvPP}(\text{O}_2)$  complex is indicated by the catalytic reduction of  $\text{O}_2$  (Figure 4B) but the catalytic turnover rate is unimpressive. Thus, the enhanced affinity for  $\text{O}_2$  that is

(15) El-Kasmi, A.; Lexa, D.; Maillard, P.; Mometeau, M.; Savéant, J.-M. *J. Am. Chem. Soc.* **1991**, *113*, 1586–1595.

(16) Steiger, B.; Anson, F. C. Unpublished experiments, 2000.

(17) Lexa, D.; Saveant, J.-M. *Acc. Chem. Res.* **1983**, *16*, 235–243.

(18) Sawyer, D. T. *Oxygen Chemistry*; Oxford University Press: New York, 1991.

realized by the addition of pivalamido "pickets" to Co<sup>II</sup>TPP is not accompanied by an improvement in catalytic activity toward the reduction of O<sub>2</sub> in aqueous or nonaqueous solution. However, it should be noted that creation of a superior O<sub>2</sub> reduction catalyst was not the goal of the synthesis of cobalt picket fence porphyrin. The objective of preparing a cobalt porphyrin with an unusually high affinity for O<sub>2</sub> in a variety of solvents was certainly fully realized.<sup>4</sup>

**Acknowledgment.** This work was supported by the National Science Foundation through a grant to F.C.A. and by the Laboratory for Molecular Sciences, an NSF supported facility at Caltech. Helpful discussions with Drs. Taek Dong Chung, Chunnian Shi, and Shouzhong Zou and with Prof. Ahmed Zewail are acknowledged with pleasure.

IC000537D